scientific reports

Check for updates

OPEN

Research on the low-temperature performance of basalt fiber- rubber powder modified asphalt mixtures under freeze-thaw in large temperature differences region

Xiaote Shi[1,2], Chundi Si[1]✉, Kewei Yan[3] & Yuefeng Zhu[4]

Accurately assessing the low-temperature performance of asphalt materials is important for asphalt pavements in cold regions with large temperature differences. This study investigates the effects of freeze-thaw cycles on the low-temperature performance of basalt fiber-rubber powder composite modified asphalt mixtures (BRMAM). The influence of basalt fibers content on the mechanical properties of asphalt binder was characterized through basic property tests and bending beam rheometer (BBR) assessments. A freeze-thaw cycle process was designed to stimulate the more realistic climate. The deterioration of low-temperature performance and freeze-thaw damage mechanism were analyzed by the splitting tensile test, three-point bending test and semi-circular bending (SCB) test. Methods suitable for evaluating BRMAM's low-temperature performance were compared and explored. The results indicate that when fiber content was about 0.3%, the reinforcement effect of basalt fibers on asphalt material was more pronounced. As freeze-thaw cycles progress, the impact of frost heave force on the cracking resistance significantly increases, while the influence degree gradually decreases. Excess fibers reduced the interfacial bond between rubber powder modified asphalt and aggregate. When fiber content is between 0.2 and 0.4%, BRMAM demonstrates optimal low-temperature performance and the least sensitivity to freeze-thaw cycles. After 30 cycles, the TSR of BRMAM with 0.3% basalt fiber even reached 47.6%.

Keywords Sustainable materials, Freeze-thaw cycles, Fiber agglomeration, Low-temperature cracking, Frost heave force

Freeze-thaw damage of asphalt pavement is a common disease in cold regions with large temperature differences[1]. On the one hand, the asphalt pavement surface layer is directly exposed to the environment, which bears the traffic load at the same time. The asphalt pavement surface layer produces temperature stress with the drop in temperature. When the stress relaxation characteristics of asphalt pavement surface layer are lower than the stress growth rate, pavement damage will gradually accumulate[2]. On the other hand, in freeze-thaw cycles environment, the water entering the pavement void will produce repeated dynamic water pressure or vacuum negative pressure suction[3]. After that, the initial internal micro-damage of pavement gradually develops into loose, cracking and other damage. Asphalt pavement damage caused by the freeze-thaw effect has seriously affected pavement service performance and life in cold regions with large temperature differences. How to accurately evaluate the effect of freezing-thawing cycles on asphalt mixture low-temperature performance is an urgent problem to be solved at present[4].

In pavement engineering examples at home and abroad, adding basalt fibers or rubber powder is one effective technical means to ease freeze-thaw problem. Basalt fibers can improve the low-temperature performance and durability of asphalt pavement[5,6]. Existing studies have shown that the addition of basalt fibers to asphalt mixtures can play a role in reinforcing asphalt mixtures, and effectively improving the high and low-temperature

[1]School of Traffic and Transportation, Shijiazhuang Tiedao University, Shijiazhuang 050043, Hebei, China. [2]Department of Rail Transit, Shijiazhuang Institute of Railway Technology, Shijiazhuang 050043, Hebei, China. [3]Department of Traffic Engineering, Shanxi Conservancy Technical Institute, Yuncheng 044000, Shanxi, China. [4]Department of Civil Engineering, California State University-Chico, Chico, CA 95929, USA. ✉email: sichundi@stdu.edu.cn

performance of mixtures[7]. Morova et al.[8] concluded that adding basalt fibers to hot-mix asphalt mixtures will significantly enhance the high-temperature stability of asphalt mixtures. Gao et al.[9] observed that basalt fibers are randomly distributed in asphalt mixtures matrix. There is a strong wrapping force of chemical bonding connections between the matrix asphalt and basalt fibers. On the other hand, rubber powder has gradually been used to modify asphalt by its environmental properties, and has also been proven to improve the low-temperature performance of asphalt binder effectively. The combination of basalt fiber and rubber powder may not only further improve the low-temperature performance of asphalt materials, but also solve the pollution problem caused by waste tires[10]. However, this aspect currently needs to receive more attention.

In terms of the low-temperature performance of asphalt mixtures, Li et al.[11] applied the SCB test to study pavement cracking at low-temperature. They used fracture energy as the evaluation index. Zhang et al.[12] proposed to use the bending strain energy at -10 °C to evaluate the low-temperature performance of asphalt mixtures and found that it had a good test effect. Zeinali et al.[13] and Qadi et al.[14] used the disk-shaped compact tensile test to explore the low-temperature crack resistance of asphalt mixtures. According to the fracture energy index, the test temperature was selected to be 10 °C higher than the low-temperature in the PG classification. The performance test of BRMAM can be carried out from a macroscopic perspective to analyze the attenuation law[15]. Although scholars have done much research on the low-temperature performance of asphalt and mixtures, no unified consensus has been formed so far.

The splitting tensile test mainly focuses on the initial failure of asphalt mixtures, but cannot reflect the properties of the material during the failure process. The three-point bending test mainly reflects the strain and material strength properties of asphalt mixtures when completely broken, but cannot accurately reflect the expansion process of cracks. The SCB test can well characterize the crack propagation process of asphalt mixtures. Therefore, it is more suitable for the object of this study. However, the SCB test has high requirements for the cutting of the initial crack, and mainly reflects the properties of asphalt mixtures working with cracks.

Therefore, it is necessary to select a more comprehensive and appropriate assessment index to deeply evaluate the low-temperature performance of BRMAM, and further explore the low-temperature performance evolution law of BRMAM under freeze-thaw cycles. According to actual pavement materials performance data under different freeze-thaw cycles, it is essential to study the evolution law of damage in the freeze-thaw process. Based on this, this paper explored the optimal basalt fibers content in asphalt binder through the basic properties test and BBR test of binder. With the help of low-temperature splitting tensile test, three-point bending test and SCB test, the deterioration law of low-temperature performance of BRMAM and the freeze-thaw damage mechanism under freeze-thaw cycles action were deeply analyzed. This paper provided technical support for the design and application of BRMAM asphalt concrete pavement in cold regions with large temperature differences. Figure 1 shows the flowchart of this study.

Materials and methods

Materials

Rubber powder modified asphalt binder

The rubber powder modified asphalt used in the study was prepared in the laboratory from heavy traffic #70 road petroleum asphalt and 15% rubber powder. The preparation process consisted of two steps. First, rubber powder was added to matrix asphalt and shear was carried out for 20 min at 175 °C at a shear rate of 2000 rpm/min. Then the mixtures were stirred at 170 °C for 30 min using a mechanical agitator to ensure the rubber powder grew and swelled in asphalt, obtaining rubber powder modified asphalt binder[16]. The technical indicators for modified asphalt binder are shown in Table 1. Besides, the rubber powder particles adopted in this study are of 30 mesh. The main component is styrene-butadiene rubber, with 7% ash, 7% extractable acetone, 54% rubber hydrocarbon, and 30% carbon black.

Basalt fibers

The basalt fibers used in the study were purchased from a local company in Tai'an, Shandong Province. The length of basalt fibers is 6 mm and the diameter is 14 μm, and other technical indicators are shown in Table 2.

As shown in Fig. 2, the basalt fibers are gray-brown and are short-cut bundle fibers. The individual filamentous basalt fibers can bond together due to the presence of an infiltrant.

Mineral aggregates

The limestone aggregates were purchased from a local stone processing plant in Hubei province, China. Coarse aggregates and fine aggregates are divided into four categories, which are 0–3 mm, 3–5 mm, 5–10 mm, and 10–15 mm. The basic properties of each type of aggregates are shown in Table 3.

The mineral powder is limestone mineral powder, and its basic properties are shown in Table 4. All indicators can meet the requirements of current technical specifications.

Test methods

Preparation of asphalt binder samples

For the actual asphalt pavement, the amount of fibers is changed as the ratio of asphalt binder to aggregates. Therefore, in this test process, the fibers content includes 0.3%, 0.6%, 0.9%, 1.2% and 1.5% (mass ratio of rubber powder modified asphalt binder). In addition, modified asphalt binder without fibers was used as the control group.

Before sample preparation, the basalt fibers were dried in an oven at 105 °C for 1 h to reduce moisture. First, the rubber powder modified asphalt binder was heated to a flowing state at 170 °C, the weighed basalt fibers were poured into the asphalt container. The mixtures were stirred for 30 min at 2000 rpm/min, making the rubber powder and basalt fiber effectively contact each other[17]. It is appropriate to add the fibers in batches and repeat

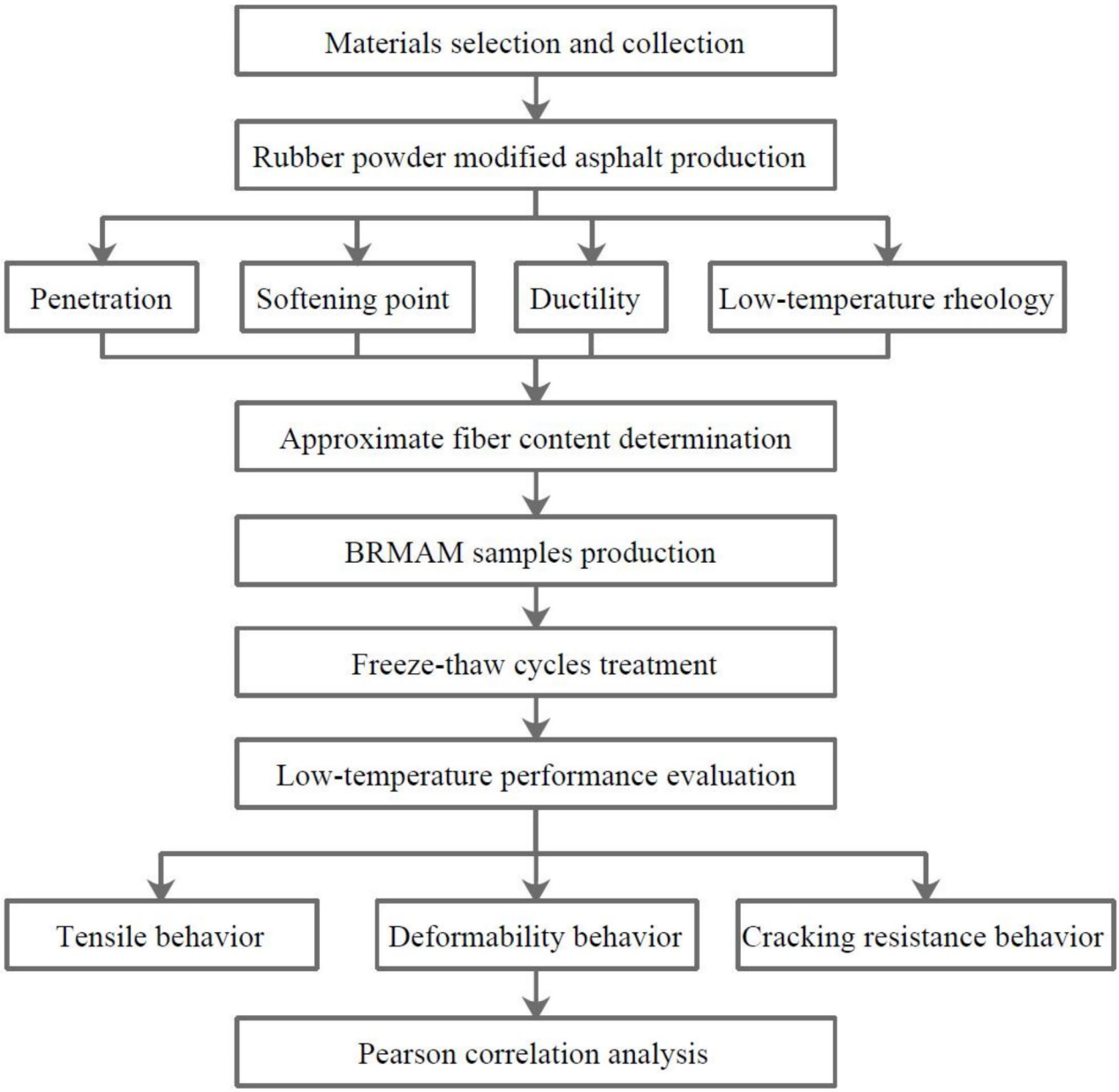

Fig. 1. Flowchart of this study.

Tested property	Units	Value	Specification
Penetration (25 °C)	0.1 mm	49.7	40–55
Softening point	°C	77.1	≥ 60
Ductility (5 °C)	cm	49.3	≥ 20
Dynamic viscosity (135 °C)	Pa·s	1.8	≤ 3
After rolling thin-film oven heating			
Weight change	%	-0.07	≤ ±1.0
Residual penetration ratio(25 °C)	cm	92.3	≥ 65
Residual ductility (5 °C)	cm	34.1	≥ 15

Table 1. Technical indicators of rubber powder modified asphalt binder.

Tested property	Units	Value
Density	g/cm^{-3}	2.69
Average length	mm	6
Fibers diameter	μm	14
Tensile strength	MPa	3050
Elastic modulus	GPa	90
Breaking elongation	%	3.12

Table 2. Technical indicators of basalt fibers.

Fig. 2. Appearance of basalt fibers.

Aggregates size	Water absorption/%	Apparent relative density/(g·cm^{-3})	Bulk relative density/(g cm^{-3})
0–3 mm	1.31	2.658	2.628
3–5 mm	1.43	2.746	2.643
5–10 mm	0.46	2.715	2.685
10–15 mm	0.51	2.739	2.706

Table 3. Main technical indicators of aggregates.

Apparent density/ (g/cm^{-3})	Moisture content/%	Hydrophilic coefficient	Plasticity index/%
2.91	0.11	0.08	2.2

Table 4. Main technical indicators of mineral powder.

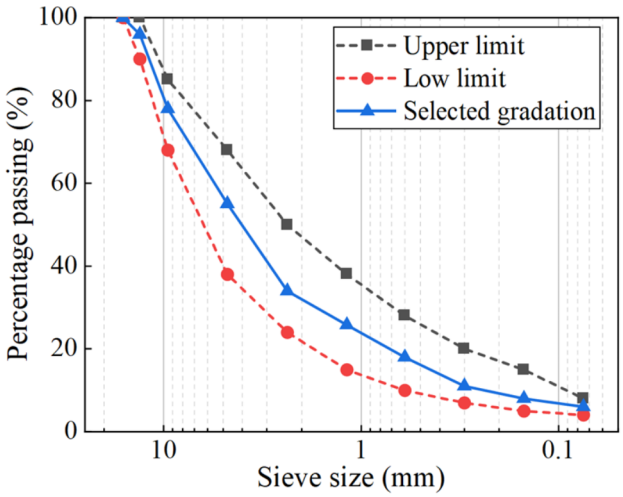

Sieve size/mm	Percentage passing/%		
	Upper	Low	Selected
16	100	100	100
13.2	100	90	95.9
9.5	85	68	77.6
4.75	68	38	55.3
2.36	50	24	34.2
1.18	38	15	25.8
0.6	28	10	17.6
0.3	20	7	11.1
0.15	15	5	8.2
0.075	8	4	5.8

(a) **(b)**

Fig. 3. Synthetic gradation of asphalt mixtures. (**a**) Gradation curves; (**b**) Gradation table.

Fiber content/%	0	0.1	0.2	0.3	0.4	0.5
Optimum asphalt content/%	4.90	5.12	5.25	5.31	5.38	5.17

Table 5. Technical indicators of basalt fibers.

the above steps until no obvious fibers are floating above the asphalt binder. Prepared test samples as soon as possible to avoid segregation.

Preparation of asphalt mixtures samples

Referring to the Technical Specifications for Construction of Highway Asphalt Pavements JTG F40-2004, the median value of the aggregate gradation for upper and lower limits prescribed by AC-13 was taken as the optimization objective. The final selected aggregate gradation is shown in Fig. 3.

Through literature research, the content of basalt fibers was determined to be 0.1%, 0.2%, 0.3%, 0.4% and 0.5% (mass ratio to aggregates), and the asphalt mixtures without basalt fibers were used as the control group. The optimal asphalt content was preliminarily estimated, and 5 groups of asphalt content were selected to form Marshall specimens around the optimal asphalt content. The optimal asphalt content was determined according to the volume index, stability and flow value of asphalt mixtures. Repeated the above steps for asphalt mixtures under each group of fibers content. The optimal asphalt content was determined as shown in Table 5.

Table 5 shows that the basalt fibers and optimal asphalt content are not consistently positively correlated. When the fibers content is low, the phenomenon of fibers adsorption asphalt is more obvious, and the optimal

Fig. 4. Production process of mixtures specimens.

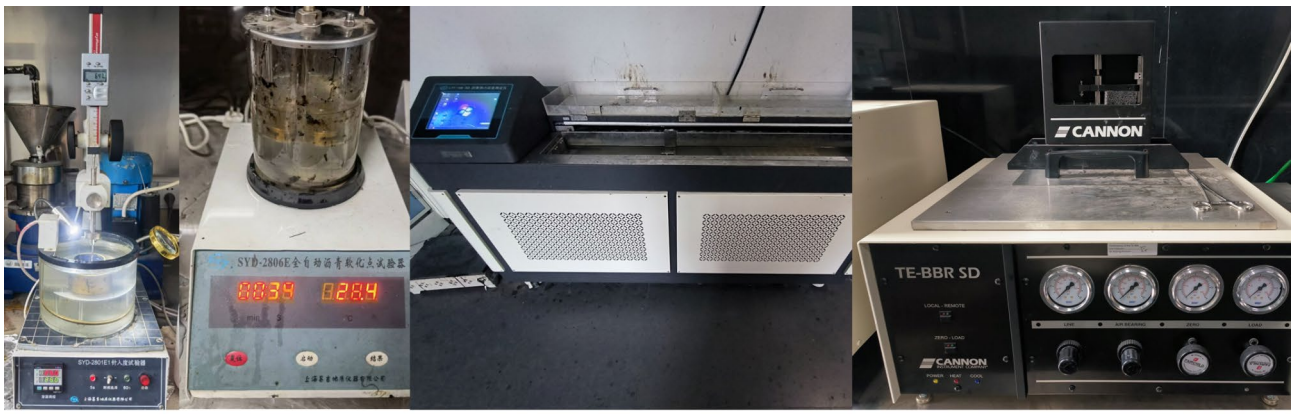

(a) **(b)** **(c)** **(d)**

Fig. 5. Properties test of binder. (**a**) Penetration test; (**b**) Softening point test; (**c**) Ductility test; (**d**) Bending Beam Rheometer test.

asphalt content increases rapidly. After continuing to increase fibers content, the excess fibers are easy to agglomerate in a limited space. They are not easy to disperse, increasing the effective surface area of fibers and a decrease in the amount of asphalt adsorbed.

The production process of mixtures specimens is shown in Fig. 4. The fibers were added to the mixtures using dry method. Add the asphalt binder after the fibers and aggregates have been stirred, and finally add mineral powder. Because basalt fiber has good heat resistance, the aggregate can enable the fiber to be better dispersed evenly[18]. The mixing temperature was controlled to 170 °C, and the total mixing time was not less than 5 min. The loose asphalt mixtures were compacted by a Marshall compactor, roller mill machine and rotary compactor according to the requirements of specimens.

Basic properties test of asphalt binder material

According to the Standard Test Methods of Bitumen and Bituminous Mixtures for Highway Engineering JTG E20-2011, the basic properties of asphalt binder were tested, as shown in Fig. 5a–c. The penetration test temperature is 25 °C. The ductility test was carried out at 5 °C, and the tensile rate was 5 cm/min.

Bending beam rheometer (BBR) test

The BBR test was conducted according to the JTG E20-2011, as shown in Fig. 5d. The flexural creep stiffness modulus S and creep rate m were measured to evaluate the low-temperature performance of binder. The BBR test temperature was set from − 6 °C to -18 °C, and the temperature interval was 6 °C.

Freeze-thaw cycles process

The study subjects were located in a cold region with large temperature differences. The average temperature in the coldest month was − 9.3 °C, the average daily minimum temperature in the coldest month was − 16.7 °C,

and the average daily maximum temperature was 9.6 °C. The temperature change on a day in the coldest month is shown in Fig. 6. It can be found that the daily minimum temperature occurred at about 8:00 am, and the maximum temperature occurred at about 16:00. The average temperature of each day is below 0 °C for more than 16 h.

In practice, after long-term freezing, asphalt pavement cannot thaw in a short period at temperatures just above freezing[19]. Therefore, to consider extreme cases, the minimum temperature for the freeze-thaw cycles test was set to be -16 °C and the maximum temperature was 10 °C. An automatic low-temperature freeze-thaw testing machine provided the freeze-thaw environment. Freezing was achieved by reducing the internal temperature of environmental chamber. The initial temperature was set to 0 °C, the cooling rate was 1 °C/h, the target temperature was − 16 °C, and the total freezing time was 16 h. Thawing was achieved by increasing the internal water temperature of environmental chamber. The thawing temperature was set at 10 °C and the thawing time was 8 h. A complete freeze-thaw cycles consist of a freezing procedure and a thawing procedure (Fig. 7).

Splitting tensile test

The splitting tensile test was carried out according to the JTG E20-2011. Before the test, the specimens were subjected to freeze-thaw cycles. When the specimens reached the expected freeze-thaw cycles times, they were removed immediately and placed in an environmental box at -10 °C together with the specimens without freeze-thaw treatment. After 4 h, the specimens were removed and tested immediately. The test was loaded using a universal testing machine. The loading rate was set to 1 mm/min[20]. The splitting tensile strength ratio (TSR) of the specimen can be calculated by Eq. (1).

$$TSR = \frac{R_{T1}}{R_{T2}} \times 100 \tag{1}$$

Where R_{T1} is the splitting strength (MPa) of the specimen after freeze-thaw cycles, R_{T2} is the splitting strength (MPa) of the specimen without freeze-thaw cycles treatment. All tests were run in quadruplicate.

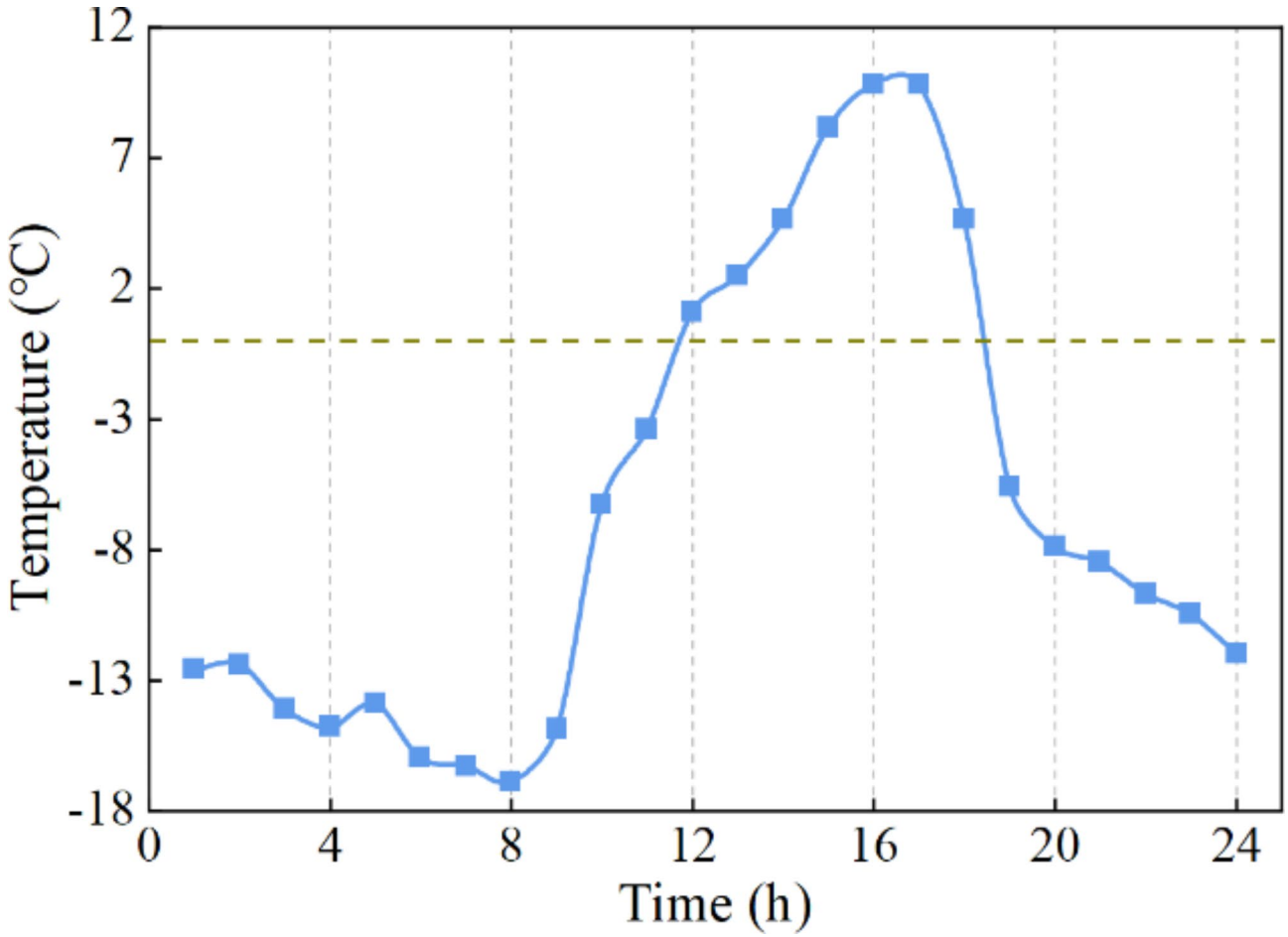

Fig. 6. Temperature changes on a given day of the coldest month.

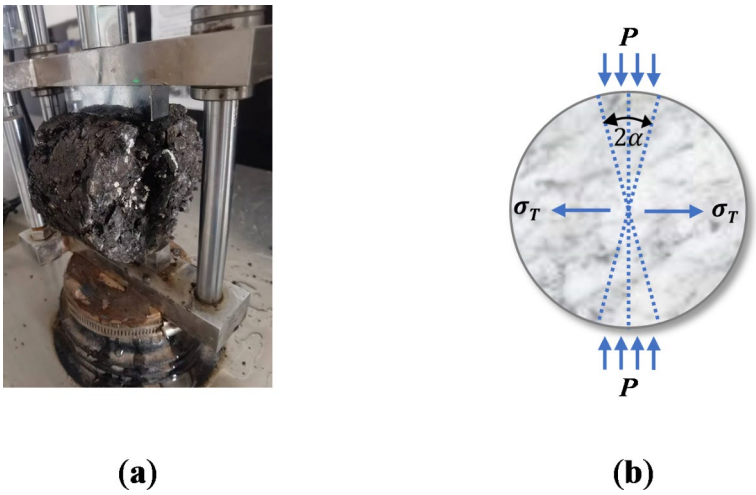

Fig. 7. Splitting tensile test. (**a**) Test instrument; (**b**) Schematic diagram of specimen force.

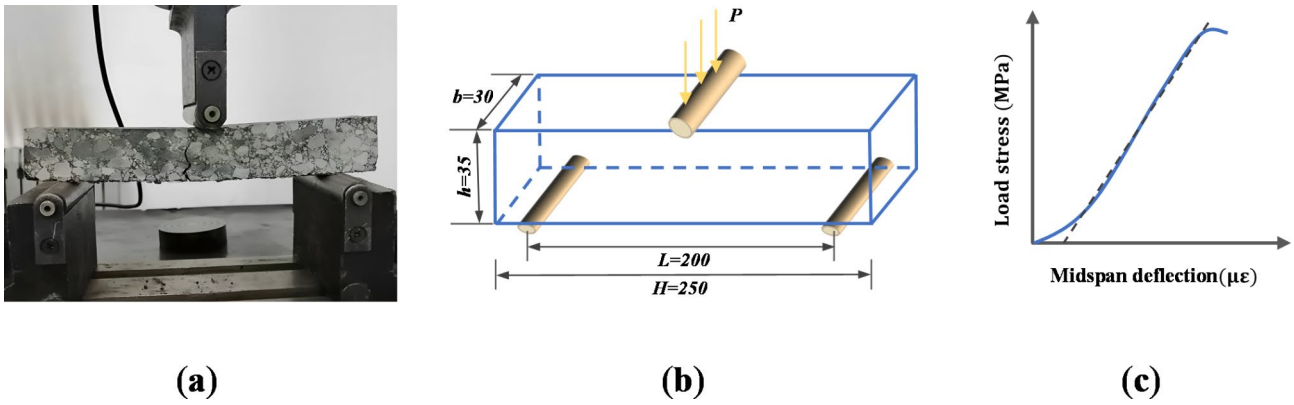

Fig. 8. Three-point bending test (**a**) Test instrument; (**b**) Schematic diagram of load situation; (**c**) Load-midspan deflection curve.

Three-point bending test

The three-point bending test was carried out according to the JTG E20-2011. Before the test, the specimens were subjected to freeze-thaw cycles. After the specimens reached the expected freeze-thaw cycles times, they were immediately removed and placed in a temperature-controlled bath at -10 °C together with the specimens without freeze-thaw treatment. After 1 h, the specimens were removed and tested immediately. A universal testing machine was used for loading until the specimen broke. Before the test, the temperature of environmental chamber was set to -10 °C and the loading rate was 50 mm/min. Analysis parameters including the flexural tensile strength R_B the maximum bending strain ϵ_B, flexural stiffness modulus S_B. These parameters can be calculated using Eqs. (2)–(4).

$$R_B = \frac{3LP_B}{2bh^2} \tag{2}$$

$$\epsilon_B = \frac{6hd}{L^2} \tag{3}$$

$$S_B = \frac{R_B}{\epsilon_B} \tag{4}$$

Where L is the fulcrum spacing (mm), P_B is the maximum load (N) when the specimen is damaged, b is the width (mm) of specimen, h is the height (mm) of specimen, d is the mid-span deflection (mm) when specimen is damaged. The schematic diagram of specimen loading position is shown in Fig. 8a,b, where the load is applied in the middle of fulcrums. Figure 8c shows the relationship curve between the load and middle span deflection of the specimen. All tests were run in triplicate.

Semi-circular bending (SCB) test

The specimen diameter was 150 mm and the height was 110 mm. The upper and lower of the molded specimen were removed by a cutting machine, and a cylindrical slice with 100 mm thickness was intercepted. A single cylindrical slice was cut along its axis into two cylinders with 150 mm diameter and 25 mm height[21]. Next, cut a slit with 5 mm long and 1.5 mm wide in the middle of each half-cylinder. The specific molding process is shown in Fig. 9a. The test method was based on the Standard Method of Test for Determining the Fracture Energy of Asphalt Mixtures Using the Semicircular Bend Geometry AASHTO TP 105–2013. Before the test, the specimens were subjected to freeze-thaw cycle treatment. After the specimens reached the expected freeze-thaw cycle times, they were immediately removed and placed into a temperature-controlled bath at -10 °C together with the specimens without freeze-thaw treatment. After 2 h, the specimens were removed and tested immediately. A universal testing machine performed loading. The loading rate was 0.5 mm/min.

Based on the fracture mechanics theory, the test mainly characterizes the anti-crack propagation performance of asphalt mixtures when working with cracks. The fracture energy is obtained by calculating the area under the load-displacement curve, which is not affected by the fracture area. A schematic diagram of the specimen loading position is shown in Fig. 9b,c. In this loading mode, specimen cracking belongs to mode I (opening crack)[22]. The typical load and displacement curves are shown in Fig. 9d. According to this curve, parameters such as fracture energy G_f (kJ/m^2), fracture toughness K_{IC} (MPa×m$^{0.5}$) and cracking resistance index CRI (m^{-1}) can be analyzed[23]. These parameters can be calculated using the following Eq.

$$G_f = \frac{W_f}{A_{lig}} \tag{5}$$

$$K_{IC} = \frac{Y_1 P_C \sqrt{\pi\, a}}{2rt} \tag{6}$$

$$CRI = \frac{G_f}{P_C} \tag{7}$$

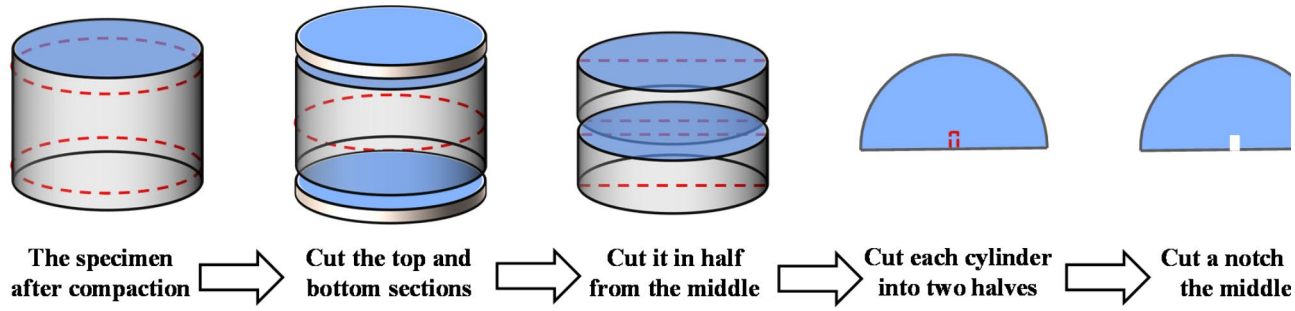

(a)

(b)

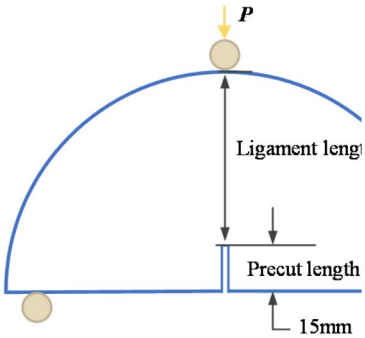

(c)

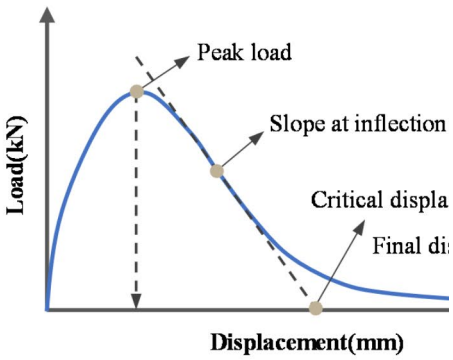

(d)

Fig. 9. SCB test. (**a**) The production process of the SCB test specimen; (**b**) Test instrument; (**c**) Schematic diagram of load situation; (**d**) Load-displacement curve.

Where: W_f is fracture work (J) and equals $\int Pdu$; P is applied load (N); u is load-line displacement (m); A_{lig} is ligament area (m2) and equals $(r\text{-}a) \times t$; r is specimen radius (m); a is notch length (m); t is specimen thickness (m); Y_1 is the normalized stress intensity factor (dimensionless); P_C is critical load (peak stress) (MN). All tests were run in quintuplicate.

Results and discussion

Basic properties test of asphalt binder

The test results of asphalt binder basic properties are shown in Fig. 10. According to Fig. 10a, the penetration of rubber powder modified asphalt binder decreases first and then gradually stabilizes with the increase of basalt fibers content. When the fibers content is 1.2%, the binder had the lowest penetration of 33.5 (0.1 mm). If the fibers content increases to 1.5%, the penetration of binder will increase slightly.

According to Fig. 10b, the softening point of rubber powder modified asphalt binder shows a gradual increase trend with the increase of basalt fibers content, and it is shown that the softening point of rubber powder modified asphalt binder can be significantly improved by adding 0.3% basalt fibers. When the basalt fibers content is 0.3%, the softening point of binder reaches 83.3 °C, which is higher than that of the control group. Further addition of basalt fibers has limited effect on improving the softening point of rubber powder modified asphalt binder.

Figure 10c shows that the ductility of rubber powder modified asphalt binder decreases with the increase of basalt fibers content. When the basalt fibers content is 0–0.3%, the decrease in ductility of binder is small. When the fibers content reaches 0.3-0.9%, the ductility of binder decreases rapidly. If the fibers content continues to increase, the ductility of binder will rarely decrease.

The main reason why basalt fibers can improve the basic properties of asphalt binder is that basalt fibers are evenly dispersed in the asphalt binder by mixing to form a network structure each other, which plays an important role in reinforcing the asphalt binder. Basalt fibers have excellent tensile properties, which can increase the crack resistance and high-temperature stability of basalt fiber modified asphalt binder, thus showing a decrease in penetration and an increase in softening point. Of course, the addition of basalt fibers will affect the cohesion between matrix asphalt, so that the complete asphalt is interspersed with fibers, thereby reducing the viscosity of asphalt itself, leading to premature fracture of the binder during the ductility test.

Low-temperature rheological property of binder

Two key indicators can be obtained through the BBR test: the flexural creep stiffness modulus S and the creep curve slope m (the curve slope of the stiffness modulus against the load time) to evaluate the low-temperature cracking resistance of asphalt binders. The S characterizes the flexibility of asphalt binder. The smaller S value, the better the flexibility of asphalt binder and the greater the allowable deformation, which indicates the better low-temperature cracking resistance. The m represents the relaxation performance of asphalt binder. The larger m value, the faster stress release speed, the stronger relaxation ability, and the better low-temperature cracking resistance. The low-temperature performance test results of basalt fiber modified asphalt binder are shown in Fig. 10d,e.

It can be seen in Fig. 10d that under the same temperature condition, the S of basalt fibers asphalt binder shows a trend of first decreasing and then increasing with the increase of basalt fibers content. When the fibers content is 0.9%, the creep stiffness of the asphalt binder is the lowest, indicating that the flexibility of asphalt binder is more evident at this time, and the maximum allowable deformation is larger. This phenomenon shows that the dispersion and uniformity of basalt fibers in asphalt binder are the best at this time, and the reinforcement effect is more significant. Under the same content condition, with the decrease in temperature, the influence of basalt fibers on the stiffness modulus of asphalt binder is more obvious. The lower temperature, the harder and more brittle basalt fiber modified asphalt binder, the higher stiffness modulus and the worse low-temperature crack resistance.

According to Fig. 10e, under the same temperature condition, with the increase of basalt fibers content, the m of asphalt binder shows a trend of first increasing and then decreasing. When the basalt fibers content is about 0.9%, the creep rate of asphalt binder is the largest. At -18 °C, the m value of asphalt binder is 0.366. If the basalt fibers content continues to increase, the creep rate of asphalt binder will decrease, which is unfavorable to the low-temperature crack resistance. However, under the the same basalt fibers content, the creep rate of asphalt binder at different temperatures is smaller than the stiffness modulus. In conclusion, specific content of basalt fibers can appropriately improve the creep rate of asphalt binder, enhance stress relaxation capacity, and reduce the risk of asphalt binder cracking. However, too much basalt fibers may lead to fibers agglomeration and other phenomena, forming a weak interface in asphalt binder and instead reducing the stress relaxation capacity of the asphalt binder.

In general, the improvement of creep rate of asphalt binder after the addition of basalt fibers is small, and the increase of the stiffness modulus is large. When fibers content is lower than 0.3%, the positive promoting effect is weaker. As the temperature decreases, the improvement of low-temperature crack resistance of asphalt binder by basalt fibers becomes much weaker. To some extent, it also reflects that the BBR test is not very objective in evaluating the low-temperature performance of modified asphalt[24].

Tensile performance of BRMAM in low-temperature

The low-temperature splitting tensile test can analyze the resist crack ability of asphalt mixtures under low-temperature conditions. When the internal stress exceeds the ultimate tensile strength of material itself, cracks will occur[25]. Figure 11a shows the change in splitting tensile strength of BRMAM samples after 1, 5, 10, 15, 20 and 30 freeze-thaw cycles under different basalt fibers content. By comparing the freeze-thaw splitting tensile

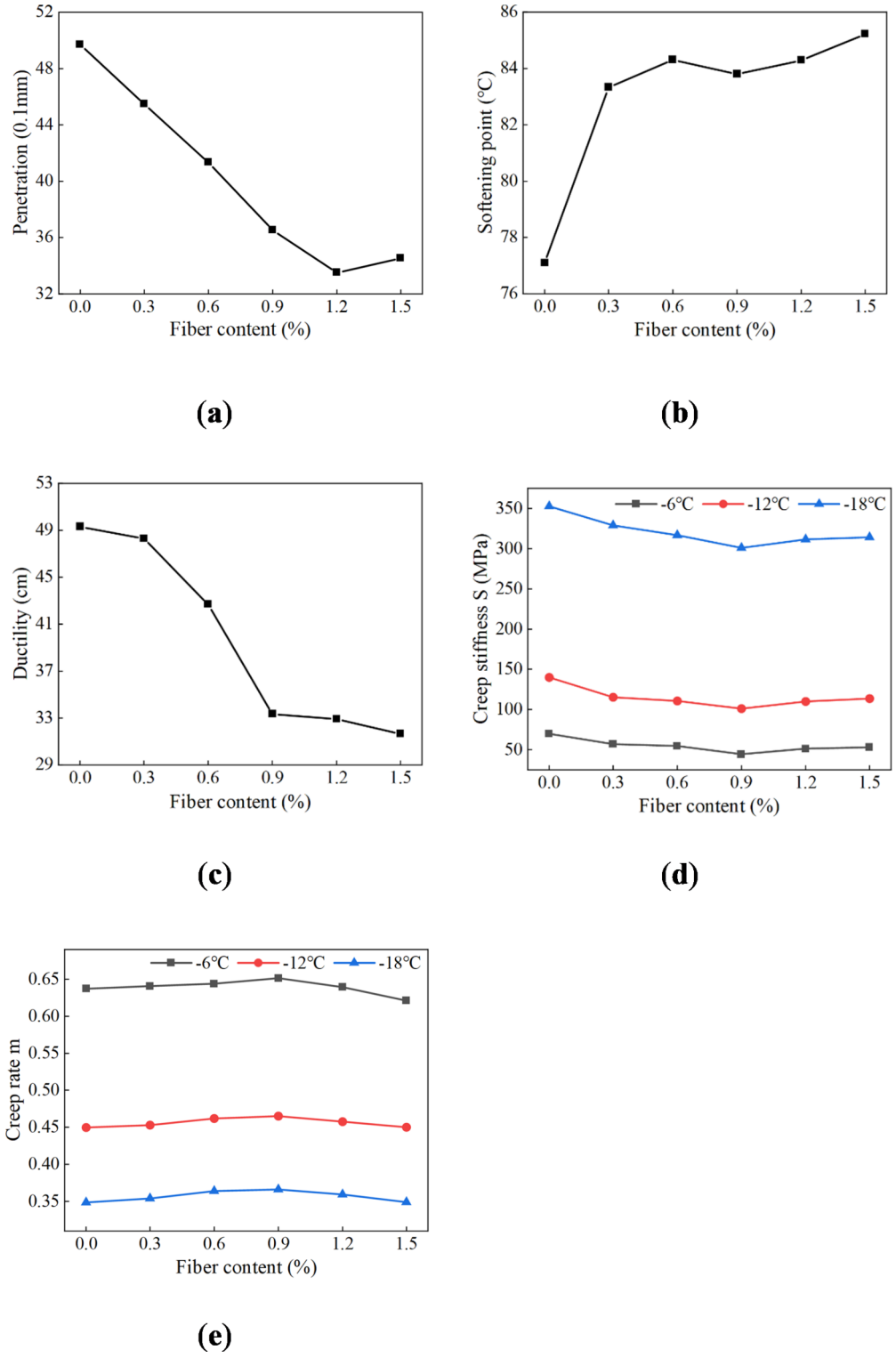

Fig. 10. Effect of basalt fibers content on the properties of asphalt binder. (**a**) Penetration; (**b**) Softening point; (**c**) Ductility; (**d**) Creep stiffness S; (**e**) Creep rate m.

strength of asphalt mixtures under different freeze-thaw cycles, it can be found that the splitting tensile strength of BRMAM with each content decreases gradually with the increase of freeze-thaw cycles. Taking basalt fibers content of 0.4% as an example, after 30 freeze-thaw cycles, the splitting tensile strength of BRMAM decreases from 4.11 MPa to 1.80 MPa. By comparing the effect of different fibers content on the splitting tensile strength of BRMAM, it can be found that the splitting tensile strength of BRMAM under each fibers content decreases with the increase of freeze-thaw cycles. However, with the progress of freeze-thaw cycles, their order of magnitude is

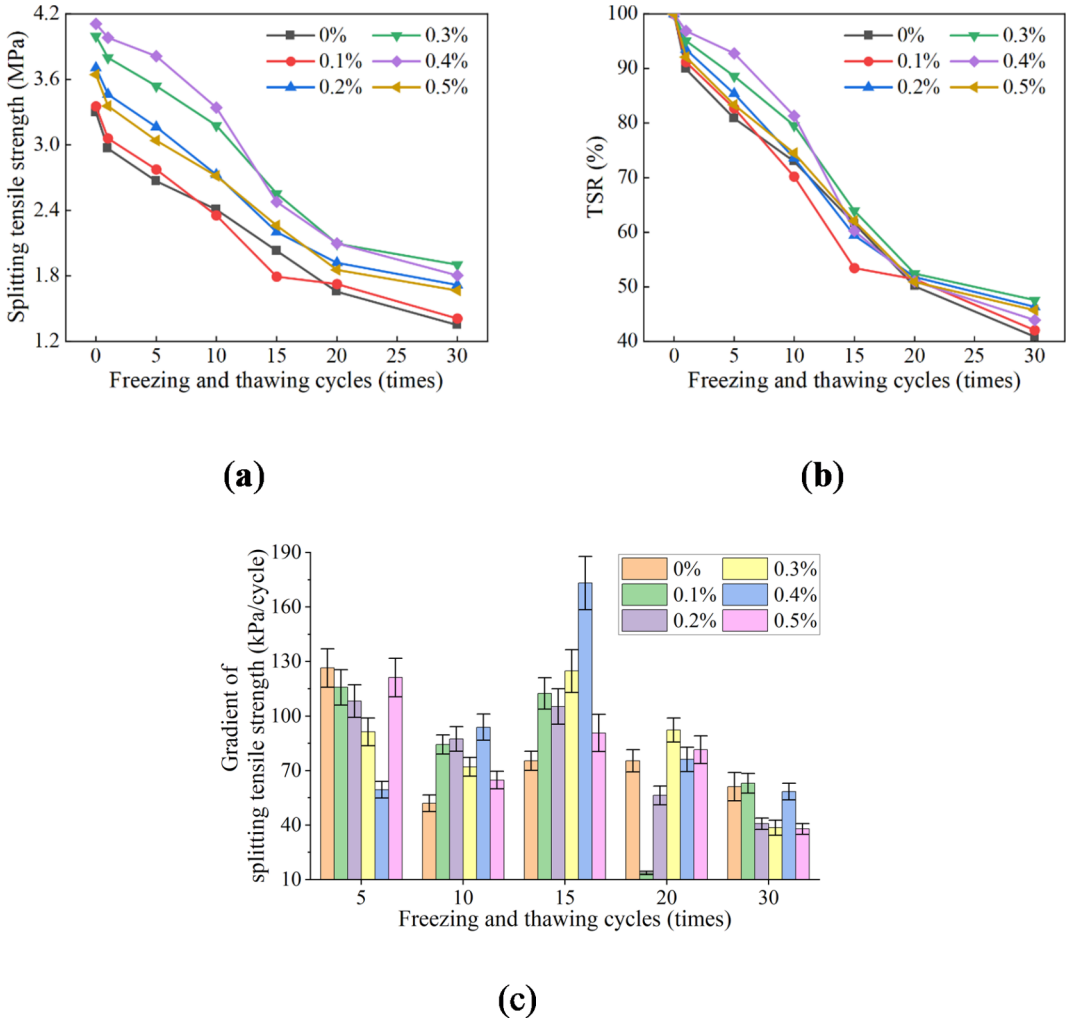

Fig. 11. Splitting tensile test results of BRMAM with different content. (**a**) Splitting tensile strength; (**b**) TSR; (**c**) Change rate of splitting tensile strength of BRMAM.

not consistent. Interestingly, the splitting tensile strength curves of three groups of BRMAM intersect, including asphalt mixtures with 0.3% and 0.4% basalt fibers, 0.2% and 0.5% basalt fibers, and no fibers and 0.1% basalt fibers, respectively.

Figure 11b shows the TSR changes of BRMAM specimens after 1, 5, 10, 15, 20 and 30 freeze-thaw cycles under different basalt fibers content. With the increase of freeze-thaw cycle numbers, the TSR of the BRMAM with each content gradually decreases. When the fibers content is 0.3%, the TSR of asphalt mixtures are 95.1%, 88.6%, 79.6%, 64%, 52.4% and 47.6%, respectively. Compared with the control group, the addition of basalt fibers can effectively improve the TSR of BRMAM, especially when the fibers content is 0.2-0.3%. After 30 freeze-thaw cycles, the TSR of the BRMAM with 0.3% fibers content was 6.7% higher than that of the control group. Continuous increase of fibers content will not bring a positive effect on the TSR. Because too many fibers cannot be evenly dispersed in the asphalt mixtures, it is easy to agglomerate and reduce the bond strength between asphalt and aggregates, resulting in structural defects inside the asphalt mixtures specimen[26]. Although the effect of fibers content on the TSR will change with the number of freeze-thaw cycles, when freeze-thaw cycles 20 times, the TSR of BRMAM under each fibers content is about 51%.

Figure 11c illustrates the change rate of the splitting tensile strength of BRMAM. It can be found that as the number of freeze-thaw cycles increases, the splitting tensile strength reduction rate of asphalt mixtures goes through two processes of increasing and decreasing. This is because when the asphalt mixtures are immersed in water, there will be a small amount of water into the mixtures through the cracks and voids. This moisture will produce dynamic water pressure and slowly penetrate the interface between the asphalt and aggregates, thereby reducing the adhesion between the two. When the temperature is reduced, the water molecules inside the mixtures are transformed from liquid to solid, which is manifested as crystallization and volume expansion, resulting in the internal structure of the mixtures becoming loose, the tensile capacity is reduced, and the maximum tensile stress can be borne is reduced. At the end of each freeze-thaw cycles, the internal water content of the mixtures increases accordingly, which reduces its strength[27]. Since the mixtures can only partially thaw at low-temperature for a short time after freezing for a long time, the mixtures are always in the process of repeated

freeze-thaw, so the reduction rate of its strength is not an obvious linear trend. When the splitting test is carried out, its failure mostly occurs in the initial dense void of the specimen, where water is easy to enter the specimen.

Deformability performance of BRMAM in low-temperature

As the environment temperature drops, the pavement will shrink and the internal stress will increase. If this shrinkage occurs fast enough, tensile stress can build up in the asphalt mixtures and may cause cracking[28]. The low-temperature bending test results of BRMAM are shown in Fig. 12. Figure 12a presents that the flexural tensile strength of asphalt concrete is significantly enhanced after the incorporation of basalt fibers. Before freeze-thaw cycles, the flexural tensile strength of asphalt concrete without basalt fibers is only 8.03 MPa. In contrast, with the addition of 0.2% basalt fibers, the flexural strength of asphalt concrete specimen increases to 8.64 MPa, with an increase of 7.6%. With the increase of freeze-thaw cycles, the flexural tensile strength of asphalt mixtures with each fibers content continues to decrease, and the reduction trend gradually slows down. This is mainly because the mixtures under the repeated action of frost heave and osmotic pressure, the asphalt binder and aggregates phase around its internal void separation, resulting in the overall bending and tensile strength of mixtures reduced. In the early stage of freeze-thaw, the mixtures inside voids play a dominant role, and provide space for the subsequent freezing heave action caused by the transformation of water to ice, so the freeze-thaw damage rate slows down in the later freeze-thaw stage. With basalt fibers content increasing, the flexural tensile strength of asphalt mixtures generally increases first and then decreases. When basalt fibers content is low, the fibers can be more evenly dispersed in the asphalt mixtures. Under vertical loads, basalt fibers by their high tensile strength, bear part of tensile stress and delay the cracking of mixtures. However, when the basalt fibers content is too large, the fibers are difficult to uniformly disperse after mixing, and even the problem of fibers clumping will occur, reducing the adhesion force of asphalt and aggregates[29].

As shown in Fig. 12b, the maximum flexural tensile strain of asphalt mixtures at each fibers content decreases with the increase of freeze-thaw cycles, and the rate decreases gradually. Because repeated freeze-thaw cycles will reduce the adhesion force of asphalt and aggregates, resulting in the asphalt producing tensile deformation

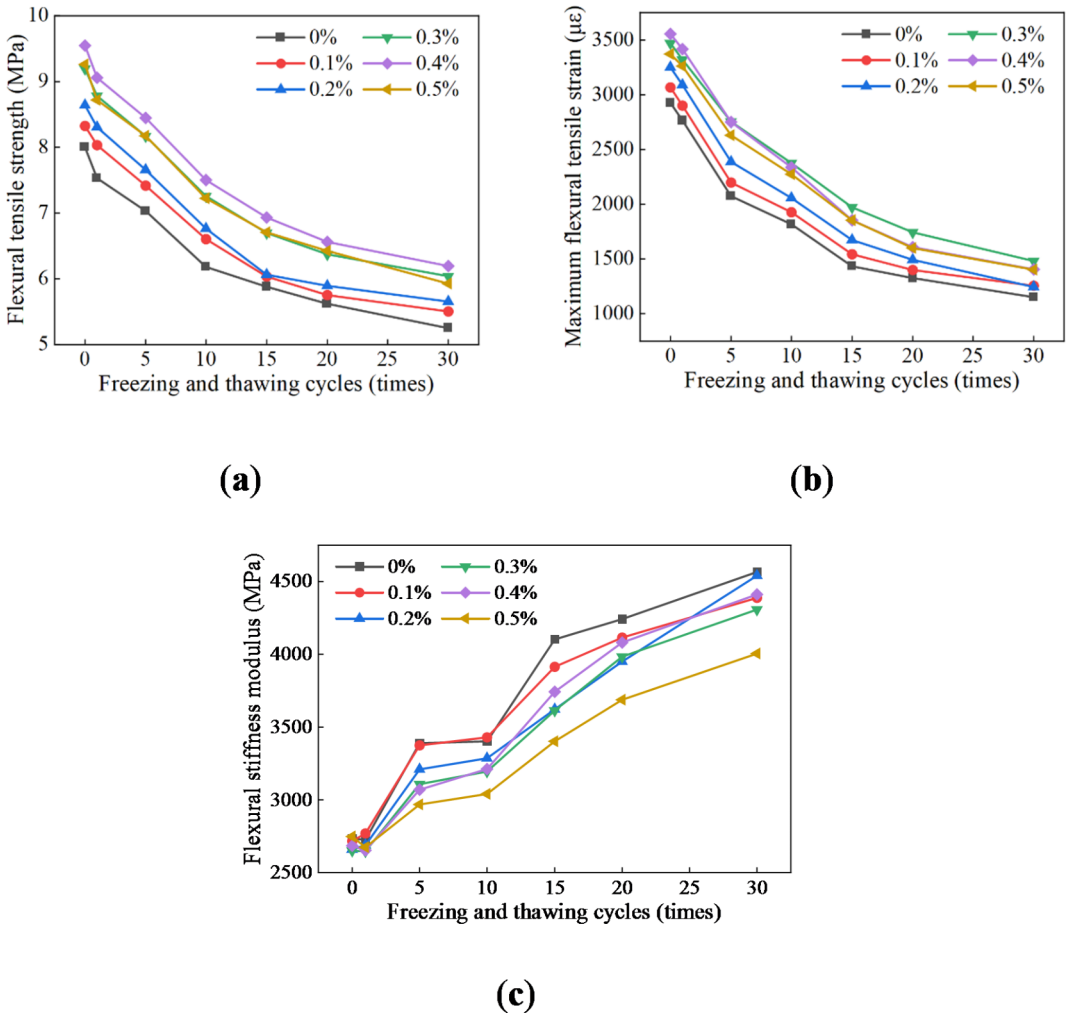

Fig. 12. Low-temperature bending test results of BRMAM with different contents. (**a**) Flexural tensile strength; (**b**) Maximum flexural tensile strain. (**c**) Flexural stiffness modulus of BRMAM with different contents.

peeling off from the aggregates surface, generating adhesive failure. The maximum flexural strain of asphalt mixtures without fibers was 2925με before freeze-thaw cycles and decreased to 1150με after 30 freeze-thaw cycles. However, the maximum flexural strain of asphalt mixtures can be increased to a certain extent after fibers are added. When the content of basalt fibers is 0.3-0.4%, the maximum flexural strain of asphalt mixtures is the largest. After 30 freeze-thaw cycles, the maximum flexural strain of the BRMAM with 0.3% fibers is 1479με, which is 1.28 times that of the control group. Compared with the flexural tensile strength, the maximum flexural strain of the BRMAM decreases more rapidly with the increase of freeze-thaw cycles. This means that BRMAM is accompanied by large deformation when bending and tensile failure, reflecting that basalt fibers can well extend the fracture path of asphalt mixtures and inhibit cracks development[30]. Although basalt fibers have a low breaking elongation, they can overlap each other in the asphalt mixture to form a three-dimensional spatial structure, which helps to reduce the internal stress of asphalt material and enables it to withstand greater deformation[31].

After freeze-thaw cycles, the flexural stiffness modulus of BRMAM with different fibers content is shown in Fig. 12c. In a complete freeze-thaw cycle, the asphalt mixtures will become hard and brittle after a long period of freezing and unable to thaw at a short period of low-temperature[20,32]. Therefore, the flexural stiffness modulus of BRMAM at each fibers content is also increasing. Interestingly, after adding basalt fibers, the flexural stiffness modulus of various asphalt mixtures decreased to varying degrees. This is due to the high oil adsorption of basalt fibers, which can stabilize part of free asphalt, so that it provides more lubrication to the mixtures, softening the asphalt mixtures[33].

Cracking resistance performance of BRMAM in low-temperature

The fracture energy and fracture toughness of BRMAM after freeze-thaw cycles can be calculated by Eqs. (6) and (7). The SCB test results of BRMAM with different fibers contents are shown in Fig. 13. Figure 13a shows that the fracture energy of each sample of BRMAM decreases after freeze-thaw cycles, especially for the first freeze-thaw cycles. After the first freeze-thaw cycles, the fracture energy of the BRMAM sample with 4% fibers content decreases the most, up to 49.4%. With the increase of freeze-thaw cycles, the fracture energy reduction rate of asphalt mixtures decreases gradually. This means that the freeze-thaw cycles reduce the crack resistance of asphalt mixtures at low-temperature, and the greater freeze-thaw cycles number, the more prone to crack disease.

By analyzing the reasons, it can be seen that the greater freeze-thaw cycles number, the greater interior damage of asphalt mixtures caused by the frost heave force generated by the phase transformation, and the more the internal microscopic cracks[34]. The increase of microscopic cracks induces the asphalt concrete failure with destructive macroscopic cracks under vertical loads. The fracture energy of asphalt concrete increases obviously when the fibers are added. This is because the addition of fibers strengthens the asphalt concrete, so the asphalt concrete needs to consume more energy from the initial crack to develop into crack failure, and it is less likely to crack. Before freeze-thaw cycles, the fracture energy of the BRMAM with 0.4% basalt fibers is as high as 4.12kJ/m^2, which is 97.1% higher than that of the control group. After several freeze-thaw cycles, the difference of fracture energy of the BRMAM with different fibers content is minimal compared with that before freeze-thaw cycles. This indicates that freeze-thaw cycles can weaken the difference in fracture energy of BRMAM caused by different fibers content. The fracture energy of asphalt concrete with different fibers content varies greatly in the early and late stages of freeze-thaw cycles, and the difference is slight in the middle stage. After 30 freeze-thaw cycles, the maximum fracture energy of asphalt concrete with 0.4% fibers content is 0.47kJ/m^2, which is 1.67 times that of the control group.

The fracture toughness of the BRMAM with different fibers contents is shown in Fig. 13b,c. Figure 13b shows that the fracture toughness of different BRMAM fluctuated greatly with the increase of freeze-thaw cycles. According to the Eq. (6), only the critical load value is different in the calculation of fracture toughness of different asphalt concrete samples, and the comprehensive performance of the sample in the whole fracture process is not considered, which induces the relationship between fracture toughness and freeze-thaw cycles to fluctuate obviously. Therefore, the relationship between them is fitted by the primary function, and the results are shown in Fig. 13c. As can be seen from the figure, with the progress of freeze-thaw cycles, the fracture toughness of asphalt concrete shows a gradual decline in general. This is caused by the decrease of adhesion between asphalt binder and aggregates interface due to freeze-thaw damage, and the decrease of cohesion in some asphalt binder[35]. In terms of curve slope, asphalt concrete without fibers has the most minor curve slope of -0.0181. However, the asphalt concrete mixed with 0.3% fibers has the highest curve slope of 0.0067. This phenomenon indicates that the addition of basalt fibers can effectively improve the fracture toughness reduction rate of asphalt concrete and help to delay the occurrence of fracture failure at low-temperature. Interestingly, when the fibers content is 0.2-0.3%, the fracture toughness of asphalt concrete does not decrease significantly. The possible reason is that freeze-thaw cycles make asphalt concrete hard and brittle. Although the specimens gradually lose their viscous properties, the maximum load they can withstand under the load action does not decrease significantly, so the fracture toughness calculated by Eq. (6) does not change significantly. This phenomenon indicates that it is not proper to analyze the low-temperature performance of asphalt concrete only by using the fracture toughness.

Research shows that the cracking resistant index (CRI) proposed by Kaseer[23] is more objective and has low variability when used to evaluate the low-temperature cracking resistance of asphalt concrete[36]. The CRI value of each asphalt concrete calculated from Eq. (7) is shown in Fig. 13d. It is obvious that the CRI of asphalt concrete at each fibers content gradually decreases with the increase of freeze-thaw cycles. This phenomenon indicates that the flexibility of asphalt concrete is weakened and the brittleness is enhanced after freeze-thaw cycles. This is consistent with the previous results. Before the freeze-thaw cycles started, the CRI of asphalt concrete without fibers was the lowest at 0.47 m^{-1}. However, the asphalt concrete with 0.4% basalt fibers had the highest CRI of

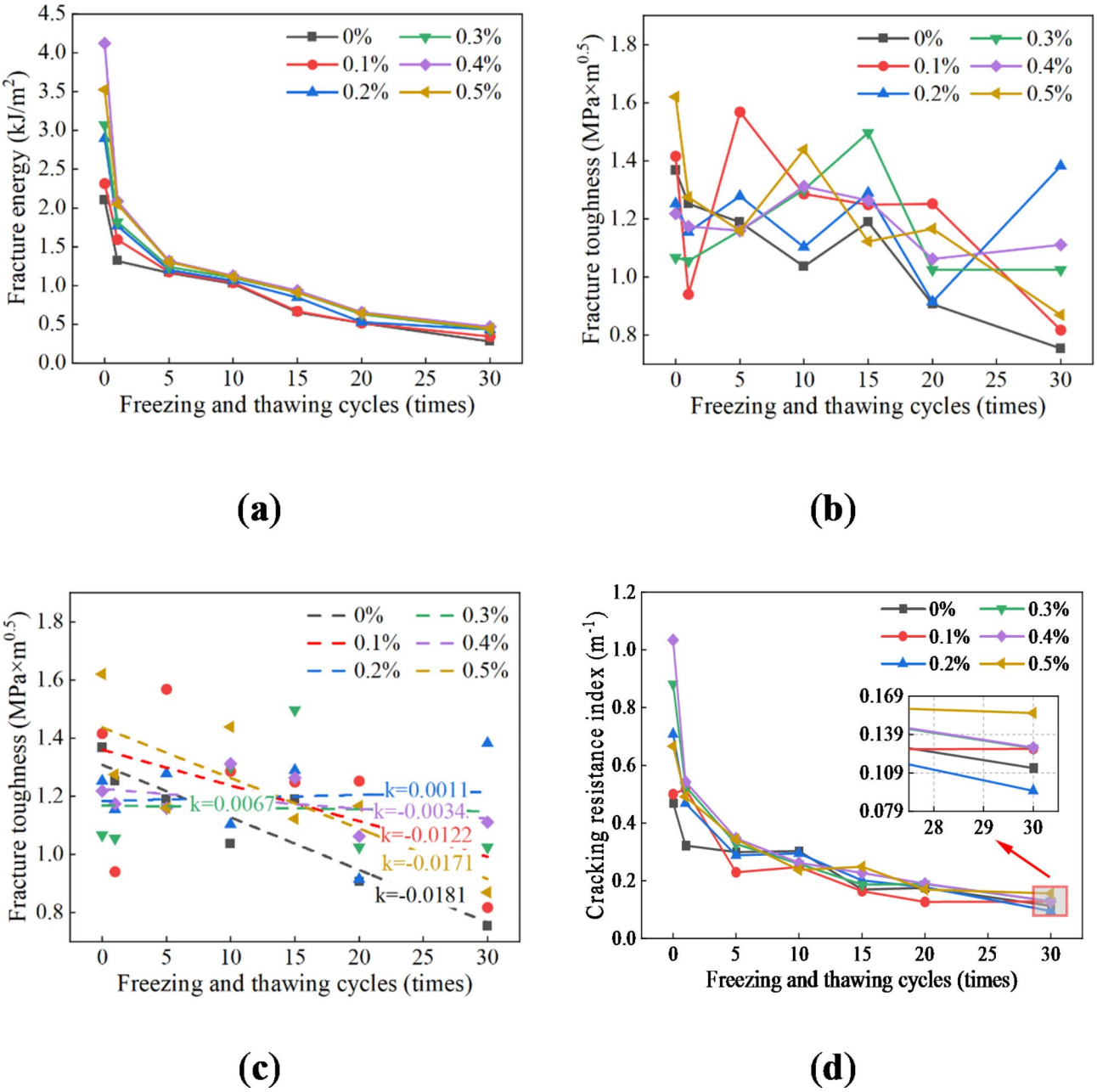

Fig. 13. SCB test results of BRMAM with different fibers contents. (**a**) Fracture energy; (**b**) Fracture toughness. (**c**) Fitting curve of fracture toughness. (**d**) CRI of BRMAM with different fibers contents.

1.03 m^{-1}, which was 2.19 times higher than that of the control group. After 30 freeze-thaw cycles, the CRI of asphalt concrete mixed with 0.2% basalt fibers was lower than that of the control group, while the CRI of other asphalt concrete was higher than that of the control group. This indicates that the addition of fibers effectively improves the low-temperature cracking resistance of asphalt concrete and makes its flexible characteristics more obvious. Of course, it can also be found that the CRI of asphalt concrete is more consistent with the trend of fracture energy changes with the increase of freeze-thaw cycles.

Correlation analysis of low-temperature performance parameters of BRMAM

After summarizing the test results of the different parameters above, Pearson correlation analysis was carried out on the low-temperature performance indicators of the BRMAM. The analysis results are shown in Fig. 14. It can be found that the fracture toughness and other indicators are weakly correlated (-0.5-0.5). The correlation between TSR and maximum flexural tensile strain, flexural tensile strength and flexural tensile stiffness modulus is higher than 0.95. It can be seen that the results of low-temperature splitting test and three-point bending test of the BRMAM are in good agreement. However, due to the attention paid to the energy consumption in the whole deformation process, the correlation of fracture energy, cracking resistance index and other indexes is low,

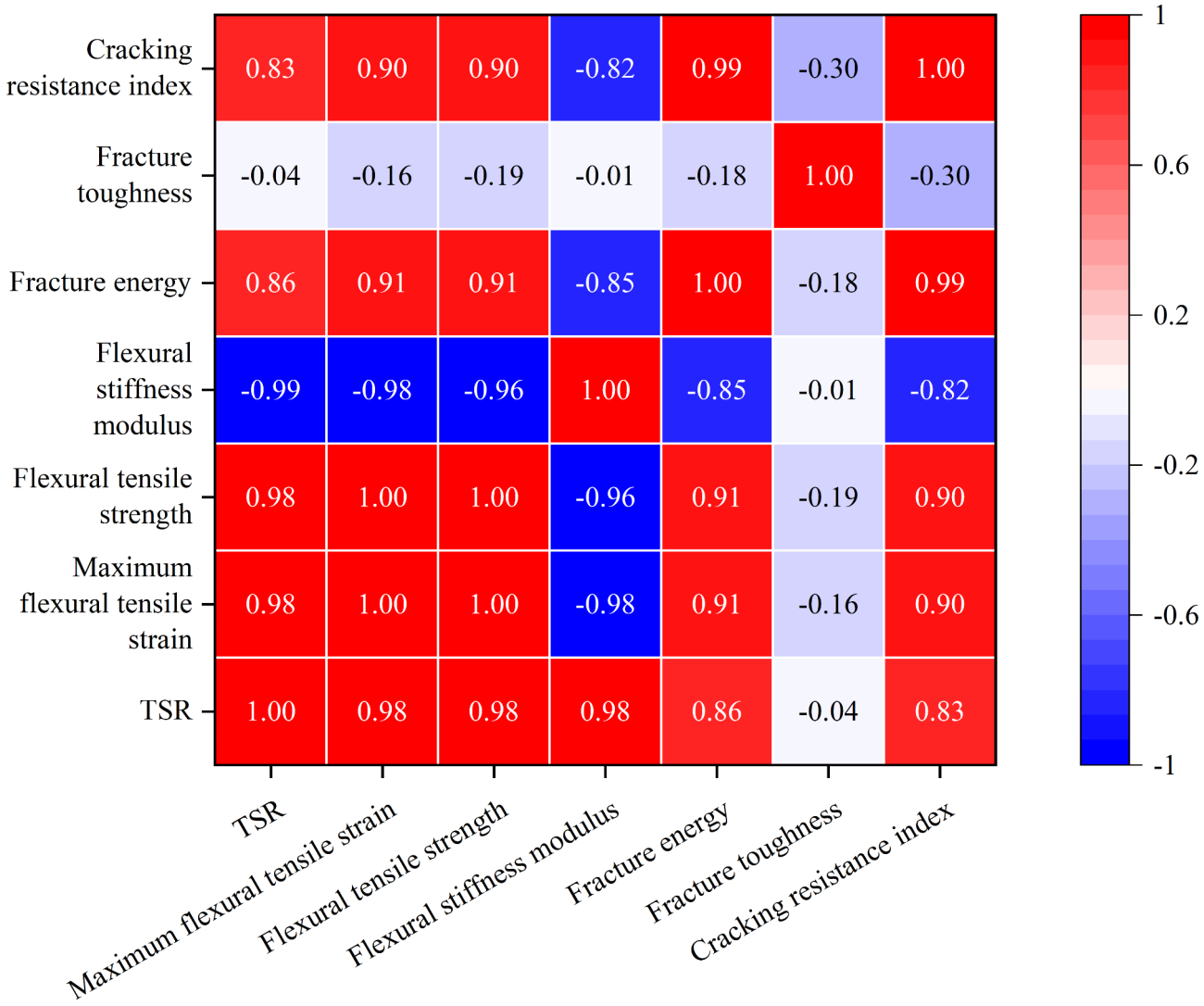

Fig. 14. Correlation coefficient matrix.

all lower than 0.95. Therefore, it is suggested that the low-temperature performance of BRMAM be evaluated by combining the semi-circular bending test with other tests.

The schematic view of the synergistic mechanism of basalt fiber-rubber powder in asphalt mixtures is presented in Fig. 15. The basalt fiber and rubber powder are evenly dispersed in the asphalt mixtures. Because of its high molecular weight and flexible molecular chain, the rubber powder dispersed in asphalt enhances the elasticity of asphalt binder. When cracks begin to expand between the aggregates, the chain segments of the rubber powder and the basalt fibers firmly pull on the asphalt binder to reduce its deformation. When the basalt fiber tends to slip, the adhesive rubber powder particles on the fiber surface increase its surface roughness, making it more difficult to slip. Generally speaking, rubber powder particles play a major role in inhibiting the growth of minor cracks, while basalt fibers play a major role in inhibiting the growth of larger cracks. The cooperation of basalt fiber and rubber powder particles improves the low-temperature performance of asphalt mixtures.

Conclusions

In this paper, the optimal content of basalt fiber in rubber powder modified asphalt binder was evaluated by the basic properties test and BBR test. Furthermore, utilizing the low-temperature splitting tensile test, three-point bending test and SCB test, the low-temperature deterioration pattern and freeze-thaw damage mechanisms of BRMAM under freeze-thaw cycles were deeply analyzed. The findings of this research provided technical insights for the design and application of basalt fiber-rubber powder modified asphalt concrete pavement in cold regions with large temperature differences. The principal research conclusions were outlined as follows.

1. When the fibers content is below 1.2%, the incorporation of basalt fibers will markedly reduce the penetration and ductility of asphalt binder, and increase the softening point of asphalt binder. The uniformly

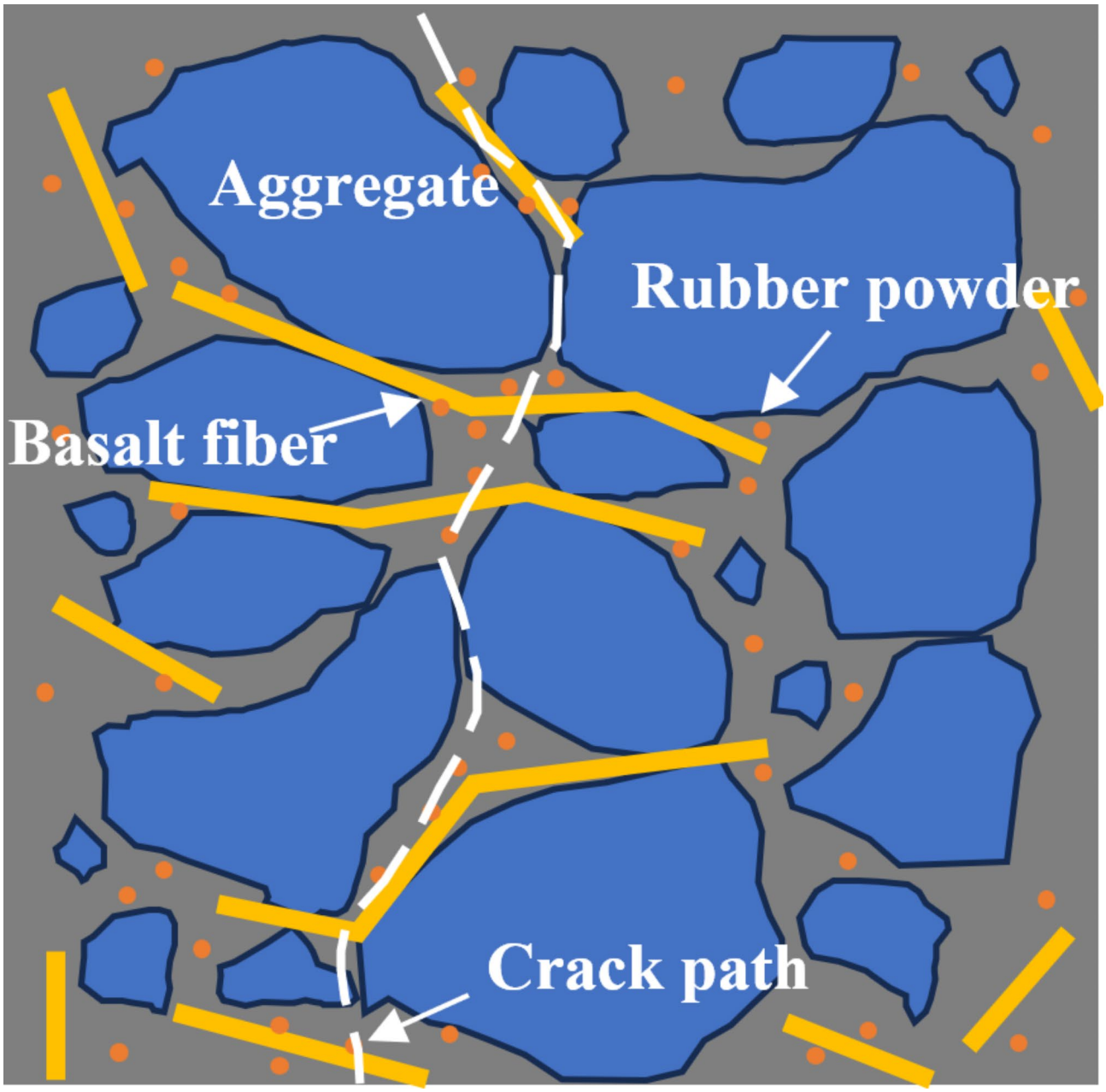

Fig. 15. Schematic view of the synergistic mechanism of basalt fiber-rubber powder in asphalt mixtures.

dispersed basalt fibers form a network structure in the asphalt material, which plays a role in reinforcing the asphalt material.

2. The splitting tensile strength and TSR of BRMAM exhibited a notable decline with the progress of freeze-thaw cycles. The decrease rate has gone through two processes increase and decrease. In the fiber content range of 0.1–0.5%, basalt fibers can substantially enhance the resistance of asphalt concrete to indirect tensile failure at low-temperature.
3. Because basalt fibers form a three-dimensional network structure within asphalt mixtures, the low-temperature bending test shows that even 0.1% basalt fibers have a good improvement on the possibility of bending and tensile failure of asphalt concrete at low-temperature. With the progress of freeze-thaw cycles, the influence of frost heave force on the low-temperature crack resistance of BRMAM gradually diminished. The incorporation of excessive basalt fibers may lead to contrary effects, which is an essential consideration for engineers.
4. Based on the SCB test, when the fibers content exceeds 0.2%, basalt fibers can significantly increase the energy consumption of asphalt concrete during the crack propagation process until complete failure. At the same time, the flexibility of asphalt concrete is enhanced and the brittleness is reduced.

5. The correlation between TSR and maximum flexural tensile strain, flexural tensile strength and flexural tensile stiffness modulus of BRMAM is very high, while the correlation between fracture energy, crack resistance index and other indicators is not very high. It is suggested that the low-temperature performance of BRMAM be evaluated by combining the semi-circular bending test and other tests.

This paper does not discuss the influence of rubber powder parameters, such as type and dosage, on the low-temperature performance of asphalt mixtures. In the future, we will combine advanced technology such as computed tomography to analyze further the collaborative improvement mechanism of rubber powder-basalt fibers parameters on the low-temperature performance of asphalt mixtures.

Data availability

The table data used to support the findings of this study are included within the article. The image data used to support the findings of this study are available from the corresponding author upon request.

Received: 1 October 2024; Accepted: 5 December 2024
Published online: 20 December 2024

References

1. Bai, R., Zhang, M., Wang, J., Li, G. & You, Z. Study on the solar albedo characteristics of pavement and embankment slope surfaces in Permafrost regions. *Sol. Energy* **237**, 352–364. https://doi.org/10.1016/j.solener.2022.04.010 (2022).
2. Shi, X. et al. Performance evaluation of BDM/unsaturated polyester resin-modified asphalt mixture for application in bridge deck pavement. *Road. Mater. Pavement Des.* **23**, 684–700. https://doi.org/10.1080/14680629.2020.1828154 (2022).
3. Kwiatkowski, K. P. et al. Modeling cost impacts and adaptation of freeze–thaw climate change on a porous asphalt Road Network. *J. Infrastruct. Syst.* **26**, 04020022. https://doi.org/10.1061/(ASCE)IS.1943-555X.0000559 (2020).
4. Cheng, Y., Yu, D., Tan, G. & Zhu, C. Low-temperature performance and damage constitutive model of eco-friendly basalt fiber–diatomite-modified asphalt mixture under freeze–thaw cycles. *Materials* **11**, 2148. https://doi.org/10.3390/ma11112148 (2018).
5. Dehghan, Z. & Modarres, A. Evaluating the fatigue properties of hot mix asphalt reinforced by recycled PET fibers using 4-point bending test. *Constr. Build. Mater.* **139**, 384–393. https://doi.org/10.1016/j.conbuildmat.2017.02.082 (2017).
6. Wu, C. et al. Effect of Diatomite and Basalt fibers on pavement performance and vibration attenuation of waste tires rubber-modified asphalt mixtures. *Math. Probl. Eng.* **2020**, e8853428. https://doi.org/10.1155/2020/8853428 (2020).
7. Chen, Y. & Li, Z. Study of road property of basalt fiber asphalt concrete. *AMM* **238**, 22–25. https://doi.org/10.4028/www.scientific.net/AMM.238.22 (2012).
8. Morova, N. Investigation of usability of basalt fibers in hot mix asphalt concrete. *Constr. Build. Mater.* **47**, 175–180. https://doi.org/10.1016/j.conbuildmat.2013.04.048 (2013).
9. Gao, C. & Wu, W. Using ESEM to analyze the microscopic property of Basalt Fiber Reinforced asphalt concrete. *Int. J. Pavement Res. Technol.* **11**, 374–380. https://doi.org/10.1016/j.ijprt.2017.09.010 (2018).
10. Tao, M., Conglin, C., Yang, Z. & Weiguang, Z. Development of using crumb rubber in asphalt modification: a review. *China J. Highw Transp.* **34**, 1–16. https://doi.org/10.19721/j.cnki.1001-7372.2021.10.001 (2021).
11. Li, X. J. & Marasteanu, M. O. Using Semi Circular bending test to evaluate low temperature fracture resistance for asphalt concrete. *Exp. Mech.* **50**, 867–876. https://doi.org/10.1007/s11340-009-9303-0 (2010).
12. Zhang, M., Huang, X. & Ren, Y. Using curvature strain energy to evaluate asphalt mixture's low temperature performance. *Petroleum Asphalt* 20–23 (2008).
13. Zeinali, A., Blankenship, P. B. & Mahboub, K. C. Comparison of Performance Properties of Terminal Blend Tire Rubber and Polymer Modified Asphalt Mixtures. In *Proceedings of the T&DI Congress 2014* 239–248 (American Society of Civil Engineers, 2014).
14. Al-Qadi, I. L. et al. Airfield and Highway Pavements (American Society of Civil Engineers: Philadelphia, 2017). ISBN 978-0-7844-8093-9.
15. Xu, H., Guo, W. & Tan, Y. Permeability of asphalt mixtures exposed to freeze–thaw cycles. *Cold Reg. Sci. Technol.* **123**, 99–106. https://doi.org/10.1016/j.coldregions.2015.12.001 (2016).
16. Lei, Y. et al. Evaluation of the effect of bio-oil on the high-temperature performance of rubber modified asphalt. *Constr. Build. Mater.* **191**, 692–701. https://doi.org/10.1016/j.conbuildmat.2018.10.064 (2018).
17. Liu, L., Huang, Y. & Liu, Z. Laboratory evaluation of asphalt binder modified with crumb rubber and basalt fiber. *Adv. Civil Eng.* **2020**, e8841378. https://doi.org/10.1155/2020/8841378 (2020).
18. Chen, Z., Chen, Z., Yi, J. & Feng, D. Application of corn stalk fibers in SMA mixtures. *J. Mater. Civ. Eng.* **33**, 04021147. https://doi.org/10.1061/(ASCE)MT.1943-5533.0003762 (2021).
19. Li, P., Zhao, J., Nian, T. & Wang, X. Research on damage constitutive relationship of continuous dense gradation asphalt mixture under freeze-thaw cycles. *Eng. J. Wuhan Univ.* **56**, 314–321. https://doi.org/10.14188/j.1671-8844.2023-03-007 (2023).
20. Li, Z. et al. Study on properties of drainage SBS modified asphalt mixture with Fiber. *Adv. Civil Eng.* **2021**, e7846499. https://doi.org/10.1155/2021/7846499 (2021).
21. AASHTO TP 105–13. *Standard Method of Test for Determining the Fracture Energy of Asphalt Mixtures Using the Semicircular Bend Geometry (SCB);* (American Association of State Highway and Transportation Officials, 2020).
22. Zarei, M. et al. Evaluation of fracture behaviour of modified warm mix asphalt containing vertical and angular cracks under freeze-thaw damage. *Int. J. Pavement Eng.* **24**, 2072500. https://doi.org/10.1080/10298436.2022.2072500 (2023).
23. Kaseer, F. et al. Development of an index to evaluate the cracking potential of asphalt mixtures using the semi-circular bending test. *Constr. Build. Mater.* **167**, 286–298. https://doi.org/10.1016/j.conbuildmat.2018.02.014 (2018).
24. Yan, K. & Wang, D. Low temperature performance index of polymer modified asphalt. *J. Build. Mater.* **23**, 479–484 (2020).
25. Wang, T., Xiao, F., Amirkhanian, S., Huang, W. & Zheng, M. A. Review on low temperature performances of rubberized asphalt materials. *Constr. Build. Mater.* **145**, 483–505. https://doi.org/10.1016/j.conbuildmat.2017.04.031 (2017).
26. Dinh, B. H., Park, D. W. & Phan, T. M. Healing performance of granite and steel slag asphalt mixtures modified with steel wool fibers. *KSCE J. Civ. Eng.* **22**, 2064–2072. https://doi.org/10.1007/s12205-018-1660-8 (2018).
27. Wang, L., Gong, N. & Xing, Y. Low temperature anti-cracking performance and temperature regulating properties of phase change asphalt mixture under freezing-thawing conditions. *J. Funct. Mater.* **47**, 4088–4093. https://doi.org/10.3969/j.issn.1001-9731.2016.04.018 (2016).
28. Hill, B. et al. Evaluation of low temperature viscoelastic properties and fracture behavior of bio-asphalt mixtures. *Int. J. Pavement Eng.* **19**, 362–369. https://doi.org/10.1080/10298436.2016.1175563 (2018).
29. Cetin, A., Evirgen, B., Karslioglu, A. & Tuncan, A. The effect of basalt fiber on the performance of stone mastic asphalt. *Periodica Polytech. Civil Eng.* **65**, 299–308. https://doi.org/10.3311/PPci.14190 (2021).

30. Guo, Q. et al. Investigation of the low-temperature properties and cracking Resistance of Fiber-Reinforced asphalt concrete using the DIC technique. *Eng. Fract. Mech.* **229**, 106951. https://doi.org/10.1016/j.engfracmech.2020.106951 (2020).
31. Honarmand, M., Tanzadeh, J. & Jandaghi, H. R. Low temperature study on the behavior of reinforced bitumen in asphalt via addition of synthesized basalt. *J. Test. Eval.* **47**, 3634–3645. https://doi.org/10.1520/JTE20180413 (2019).
32. Pei, Z. et al. Effects of fiber diameter on crack resistance of asphalt mixtures reinforced by basalt fibers based on digital image correlation technology. *Materials* **14**, 7426. https://doi.org/10.3390/ma14237426 (2021).
33. Zhang, J., Huang, W., Zhang, Y., Lv, Q. & Yan, C. Evaluating four typical fibers used for OGFC mixture modification regarding drainage, raveling, rutting and fatigue resistance. *Constr. Build. Mater.* **253**, 119131. https://doi.org/10.1016/j.conbuildmat.2020.119131 (2020).
34. Kavussi, A., Karimi, M. M. & Ahmadi Dehaghi, E. Effect of moisture and freeze-thaw damage on microwave healing of asphalt mixes. *Constr. Build. Mater.* **254**, 119268. https://doi.org/10.1016/j.conbuildmat.2020.119268 (2020).
35. Karimi, M. M., Dehaghi, E. A. Behnood, A. A. Fracture-based, approach to characterize long-term performance of asphalt mixes under moisture and freeze-thaw conditions. *Eng. Fract. Mech.* **241**, 107418. https://doi.org/10.1016/j.engfracmech.2020.107418 (2021).
36. Song, W. & Wu, H. Advances in fracture mechanics studies on fracture resistance and research methods of asphalt concrete. *Mater. Rep.* **37**, 93–103. https://doi.org/10.11896/cldb.22050119 (2023).

Acknowledgements
The authors are grateful to the Natural Science Foundation of China for providing the financial support.

Author contributions
Conceptualization, Y.Z. and C.S.; methodology, X.S. and Y.Z.; test X.S.; writing, X.S. and C.S.; validation, K.Y.; revising, Y.Z. and C.S. All authors reviewed the manuscript.

Funding
This research was funded by [Natural Science Foundation of China] grant number [11972237, 52378455].

Declarations

Competing interests
The authors declare no competing interests.

Additional information
Correspondence and requests for materials should be addressed to C.S.

Reprints and permissions information is available at www.nature.com/reprints.

Publisher's note Springer Nature remains neutral with regard to jurisdictional claims in published maps and institutional affiliations.